NIGERIAN JOURNAL OF ENGINEERING RESEARCH UNICROSS (NJERU)

Volume 1, Issue 2, 1st June, 2024

Modelling And Simulation of a Field-Oriented Controlled Hybrid Stepper Motor Using Self Tuning Fuzzy-Pid Controller

Mike O. Ejunka [a,*], Ogri J. Ushie [b], Gertrude A. Fischer [c]

[a,c] Department of Electrical and Electronic Engineering, University of Cross River State, Calabar, Nigeria

[b] Department of Electrical and Electronic Engineering, University of Calabar, Nigeria

[*]Corresponding author: mikeejunka@gmail.com

Received: 20th August, 2024 Reviewed: 28th August, 2024 Accepted: 16th September, 2024

Abstract:
This study presents a field-oriented control (FOC) scheme for a two-phase Hybrid Stepper Motor (HSM) using a self-tuning fuzzy-PID controller. A MATLAB/SIMULINK model is developed to analyze the transient performance of the HSM. The drive system consists of an H-bridge PWM inverter, hysteresis current controller, PID controller, Park transformation block, and HSM subsystems.The self-tuning fuzzy-PID controller regulates the HSM speed, while the hysteresis current controller manages phase currents. Simulation results verify the proposed FOC drive model's effectiveness, demonstrating fast dynamic performance in both transient and steady-state operation with a 0.1 Nm load. The HSM model ST601 exhibits precise positioning and speed control.

Keywords: Stepper Motor, Controllers, Self-Turning, Hybrid, Speed Level.

I. INTRODUCTION

A hybrid stepper motor (HSM) is a DC motor used in numerous industrial areas due to its properties of high torque at low speeds and simple position control in open-loop operation. [1,2,3] The motor is mainly used in applications where the precision requirements of the drive are not critical and the torque requirements are modest. The motor implemented in many applications requires high-level precision control in the open- or closed-loop control method. Robots, Computer Numerical Control (CNC) machines, basic automation setups, robotic arms, scanners, printers, machinery with low torque requirements such as 3D printers, high-end office equipment, and hard disc drives are some of the applications where stepper motors can be applied. [1,2,5] Stepper motors are widely used in industrial and consumer applications. The ability to convert discrete pulse series into rotor angular displacement enables the stepper motor to operate in open-loop mode. Generally, stepper motors operate in an open loop, i.e., there is no rotor position feedback to the controller. Therefore, the rotor position and speed are controlled by the pulse amount and pulse frequency, respectively [4,5,8]. Permanent Magnet Stepper motors (PMSM) are an integral part of many industrial and commercial products where precision movement is required. One of their biggest advantages is that they can be driven to an exact position without the need for positional feedback, as long as the speed, acceleration, and load are low enough [1,3]. Due to the lack of feedback requirements, the most common control method for stepper motors is open-loop control, where the phase currents of the motor are driven in such a way that they produce sequential steps [10]. The stepper motor is made up of two major components: a stator and a rotor. The stator (the static part) consists of a number of electromagnets, connected in two or more separate phases. The rotor of an HSM is made of a permanent magnetic material constructed in a teethed fashion. The teeth introduce an effect called the minimal reluctance effect, which states that the magnetic fields want to cross as little permeability as possible. Hence, the easiest path for the magnetic fields to travel will be when the teeth on the rotor align perfectly with the teeth on the stator, introducing added torque. [2,7,8]. The solid rotor, which has no physical contact with the stator, and the moving part, which contains no windings, make the construction of the HSM very durable and not subject to much wear during operation. From this basic construction, movement will be created by inducing magnetic fields in the stator by driving opportune currents through the electromagnets. This will cause the magnetic rotor to start moving and aligning its teeth with the stator teeth. This movement is what is referred to as a step. Using this behavior, desirable rotational movement can be found by exciting the phases in turns to create a continuous movement to a desired position. Instead of fully exciting both coils simultaneously in the full-stepping strategy or individually in the half-stepping strategy, a partial excitation of the coils is introduced to allow the rotor to align at even smaller increments between the poles. This method is called the micro-stepping or wave-stepping method. For example, if phase *A* is excited with 75% of the maximum current magnitude, while phase *B* is excited with 25% of the current magnitude, the rotor will align itself proportionally between the two poles. With this method, the resolution of the stepper motor is increased to match the resolution of the current generation through the coils. This method introduces a higher resolution of the motor steps, which is essentially dependent on the resolution of the current controller supplying current to the motor phases. There is an increase in the number of stop positions to an arbitrary amount, as well as keeping the torque more stable throughout the revolution of the motor. [9].

A common method of micro-stepping is called sine/cosine micro-stepping, in which the currents supplied to the coils will be sinusoidal with a 90-degree phase shift between them. The control signals now look more like cosine waves and sine waves and require more complicated hardware to create, such as an inverter to create a PWM signal. The major drawback with micro/wave stepping, as well as that of full-stepping and half-stepping strategies, is that they are all open-loop methods, as they are prone to losing steps. [10,11,16]. This means that the commanded position does not match the actual position. Steps will be lost when the angle between the stator field and the rotor position becomes greater than 180 electrical degrees, as this causes the quadrature force (the force that produces torque on the rotor) to change sign and the motor to snap back to the previous position without it being registered by the open loop driver. If the cause of the large angle is transient, the motor will continue operating normally after the snap-back event, but with an offset of one or more steps. Situations where this occurs are when the load torque applied to the motor exceeds the driving torque. This can be caused by a too heavy load. Field-oriented control (FOC) is a common closed-loop control strategy for hybrid stepper motors. It uses the park transformation (into *a DQ-reference* frame) to control the position of the rotor by keeping the direct-axis current (Id) at zero and then controlling the quadrature-axis (Iq) current. Depending on the implementation, it might also control the magnitude of the current to increase the torque produced. The *dq* transformation is sometimes used [12,13,15]. When applying field-oriented control (FOC) strategies to the hybrid stepper motor (which will be introduced in Chapter 3), the transformation translates the fixed ab-coordinate system aligned with the phases A and B of the stator, instead of rotating along with the rotor of the motor. The two dq-coordinates are the direct-axis component, which is aligned with the magnetic flux vector of the permanent magnet rotor, and the quadrature-axis component, which is perpendicular to the direct-axis coordinate, leading the direct axis by 90 electrical degrees [13,14,18].

2. METHODOLOGY

Initially, the electrical equations of the system (the voltage in the two phases) can be modeled as in [18,19]. The voltage sources ea and eb represent the motor back EMF (electromotive force) voltages, which are sinusoidal functions of the rotor position. The back-EMF voltages in the electric equations can be rewritten according to (Samokhvalov, 2015). For phase A, the back EMF becomes

$$\frac{d\,\lambda_{am}}{dt} = e_a = -\omega_r K_m.\sin(N_r\theta_r) \quad (1)$$

Note that at the reference position is zero, the north pole on the rotor is fully aligned with A-axis pole so that the A-phase back EMF is then zero. For phase B, the back EMF becomes

$$\frac{d\,\lambda_{bm}}{dt} = e_b = \omega_r K_m.\cos(N_r\theta)\ \} \quad (2)$$

The stator voltage equations for phase A and phase B are given in (3) and (4), respectively. The voltage equations depend on the impedance of wires, mutual flux linkages, and the current throughout the phases of the motor.

The voltage equations of a two-phase hybrid stepper motor are described as;

$$V_a = R_a I_a + L_a \frac{d\,I_a}{dt} - \omega_r K_m . \sin(N_r \theta_r) \quad (3)$$

$$V_b = R_b I_b + L_b \frac{d\,I_b}{dt} + \omega_r K_m . \cos(N_r \theta) \} \quad (4)$$

The dynamic equations of HSM can be written in state space form as follows

$$\frac{d\,I_a}{dt} = \frac{1}{L_a}[V_a - R_a I_a + \omega_r K_m \sin(N_r \theta)] \quad (5)$$

$$\frac{d\,I_b}{dt} = \frac{1}{L_b}[V_b - R_b I_b - \omega_r K_m \,\mathrm{Cos}\,(N_r \theta)] \quad (6)$$

The derivative of the angular position gives the rotor speed [21,22,23].

$$\frac{d\,\theta_r}{dt} = \omega_r \quad (7)$$

The maximum flux per pole (λ_m) and the number of pole pair (N_r) are constant, therefore

Motor constant is given as

$$K_m = \lambda_m . N_r \quad (8)$$

The mechanical Model equation based on Newtonian physics for rotating bodies relating the developed torque is written as

$$T_e = \left[J \frac{d\omega_r}{dt} + B\omega_r + T_L\right] \quad (9)$$

In HSM. The magnitude of force that created torque on rotor (shaft) is determined by currents and mechanical angle made by rotor scaled by motor constant is known as developed or electromagnetic torque given as

$$T_e = [-K_m . I_a \sin(N_r \theta) + K_{m.} I_b \cos(N_r \theta)] \quad (10)$$

Field oriented control strategy is applied when the control system is described in D Q coordinates as follows;

(b) (a) Model of Two- Phase Hybrid Stepper Motor in D-Q Reference Frame

Park transformation matrix (K) is given as

$$K = \begin{bmatrix} \cos(N_r \theta) & \sin(N_r \theta) \\ -\sin(N_r \theta) & \cos(N_r \theta) \end{bmatrix} \quad (11)$$

By applying Park in (3) to phase voltage supply (Va, Vb), we obtain voltage supply in d-q synchronous frame as;

$$\begin{bmatrix} U_d \\ U_q \end{bmatrix} = \begin{bmatrix} \cos(N_r \theta) & \sin(N_r \theta) \\ -\sin(N_r \theta) & \cos(N_r \theta) \end{bmatrix} \begin{bmatrix} V_a \\ V_b \end{bmatrix} \quad (12)$$

The reference phase currents in alpha reference frame can be obtained by applying inverse Park transformation matrix to FOC dq reference currents as follows;

$$\begin{bmatrix} I_a \\ I_b \end{bmatrix} = \begin{bmatrix} \cos(N_r \theta) & -\sin(N_r \theta) \\ \sin(N_r \theta) & \cos(N_r \theta) \end{bmatrix} \begin{bmatrix} I_d \\ I_q \end{bmatrix} \quad (13)$$

The voltage equations referred to alpha -beta reference frame in (3), (4) and (10) are applied with Park transformation matrix in (11) and they are transformed into D-Q (synchronous reference frame) as shown below. Where $R_d = R_q = R_s$, $L_d = L_q = L_s$ for non- salient motor.

$$U_d = R_s I_d + L_s \frac{dI_d}{dt} - L_s N_r \omega_r I_q \quad (14)$$

$$U_q = R_s I_q + L_s \frac{dI_q}{dt} + L_s N_r \omega_r I_d + K_m \omega_r \quad (15)$$

In FOC strategy, $I_d = 0$.

The electromagnetic torque is expressed as [24]

$$T_e = K_m . I_q = \lambda_m . N_r . I_q \quad (16)$$

Detent torque is given as

$$T_d = T_{dm} \sin(4. N_r \theta) \quad (17)$$

The complete state space equations for DQ Model of HSM is obtain from (4), (5), (7) and (8) given as

$$\frac{d\,I_d}{dt} = \frac{1}{L_s}\left[U_d - R_s I_d + L_s N_r \omega_r I_q\right] \quad (18)$$

$$\frac{d\,I_q}{dt} = \frac{1}{L_s}\big[U_q - R_s\,I_q - L_s N_r \omega_r I_d - K_m \omega_r\big] \qquad (19)$$

$$\frac{d\omega_e}{dt} = \frac{1}{J}\big[K_m I_q - B\omega_e - T_L - T_{dm}\sin(4.N_r\theta)\big] \qquad (20)$$

$$\frac{d\theta_e}{dt} = \omega_e \qquad (21)$$

The electrical position (Θ_e) of current vector between two closest poles of HSM is related with mechanical rotor position (Θ_r) as [25,26,27].

$$\theta_e = N_r\,.\,\theta \qquad (22)$$

The detent torque in (17) is considered zero in this work, since the detent torque (Td) does not significantly affect the torque produced by the motor and it is ignored [25,26,27].
The rotor angular position in radians is obtained from (22) as;

$$\theta_r = \theta_e\,.\,\frac{1}{N_r} \qquad (23)$$

The number of pole pairs (N_r) of the rotor is given in (22)

$$N_r = \frac{360}{2\,k\,\emptyset_s} \qquad (24)$$

Where k is the number of phases of voltage supply to stepper motor and $\emptyset_s$ is the step angle in degrees.

3. RESULTS AND DISCUSSION

The hybrid stepper motor (HSM) modelled as shown in figure 1 was simulated in MATLAB/SIMULINK software to confirm the analysis in this work. The proposed closed loop drive system is based on field-oriented control (FOC) with an adaptive fuzzy-PID controller and a conventional PID controller, where variable reference speeds were set at 20 rad/s, 50 rad/s, and 30 rad/s and simulated. The simulation results for a simulation duration of one to 1.4 seconds are presented in this chapter.

4.1 Adaptive Fuzzy-self tuning-PID- operation of Two-Phase Hybrid Stepper Moto

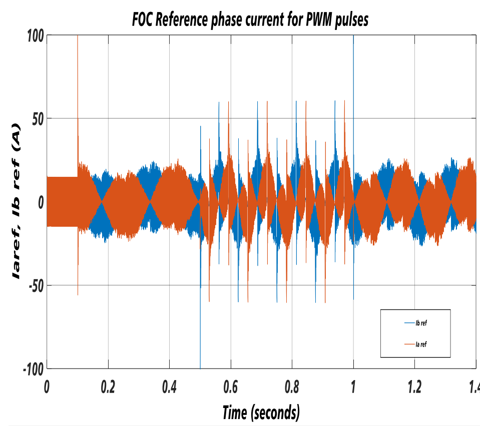

Figure 1: Field Oriented Control Referenced phase currents for variable reference speed tracking

Figure 1 shows the reference phase current that is fed to the hysteresis current controller for the generation of switching pulses. The referenced phase currents (Ia and Ib) for variable reference speed tracking have an amplitude magnitude of 10–16 A with spikes at certain instances. Also, the higher the speed value, the higher the reference current spike magnitude.

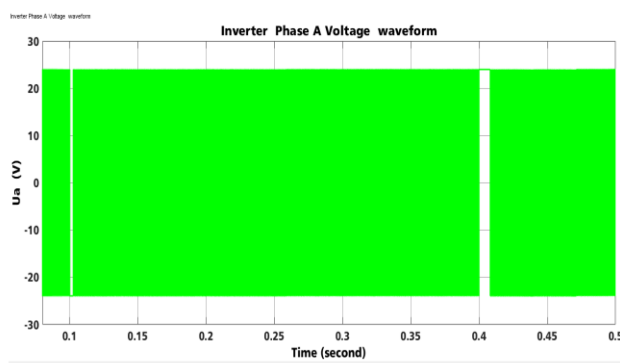

Figure 2: Inverter Phase A voltage waveform

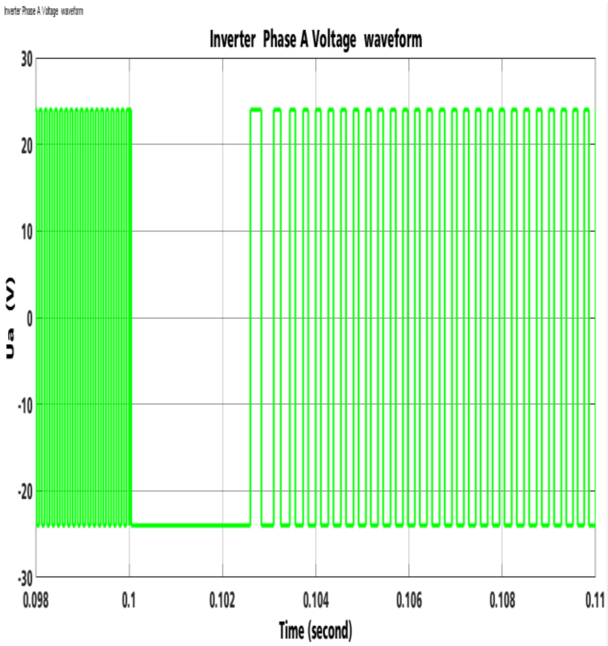

Figure 3: Inverter Phase B voltage waveform

Figures 2 and 3 depict the H-Inverter Phase A output voltage waveform, which is supplied to the field-oriented controlled two-phase hybrid stepper motor. The output waveform is generated from the pulse with modulation technique (PWM) H-Bridge Inverter Phase. The output waveform has a peak amplitude of +-Vs (+-24v) with a variable duty cycle ratio, from (a) voltage magnitude drops to -24v at every instant within a duration of 0.0025 seconds.

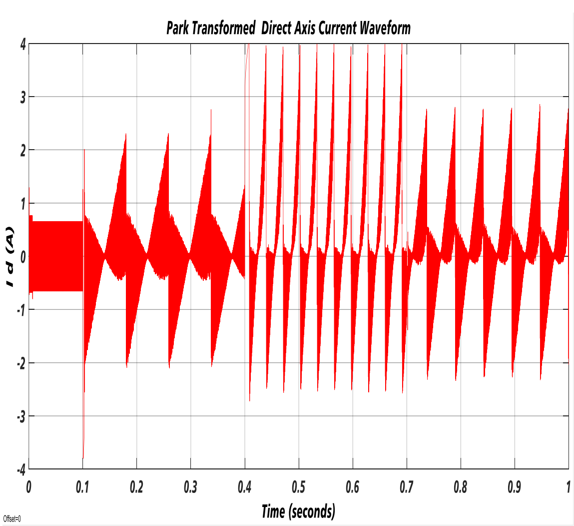

Figure 4: Motor direct-axis Current (Id) Response from Park Transformation Block

Figure 3 depicts the direct-axis current (Id) response from the Park transformation block in the HSM model. It shows (Id) has approximately **zero magnitude** with minor ripples, notably when the motor step speed is at 50 rad/s. This is expected as a field-oriented control strategy is implemented to maintain the direct-axis current (Id) value at zero amperes.

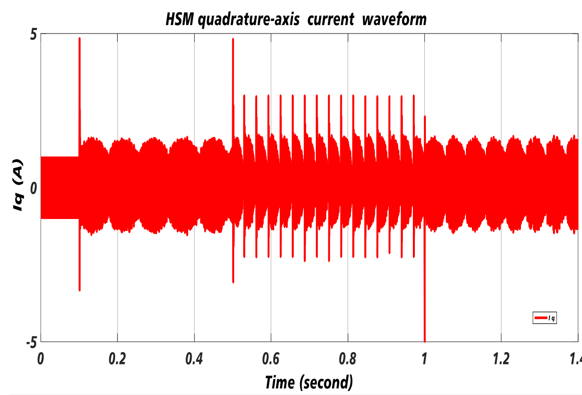

Figure 5: Motor quadrature -axis current Waveform

Figure 5 depicts the quadrature-axis current (Id) response from the Park transformation block in the HSM model. It shows (Iq) has approximately 2 amplitudes with spike at every instance of step change in reference speed (0.1 sec, 0.5 sec, 1.0 sec). The magnitude of the current increases at certain instances during a higher speed period between 0.5 and 1.0 seconds. Higher speeds require high torque, and the Iq is a function of torque.

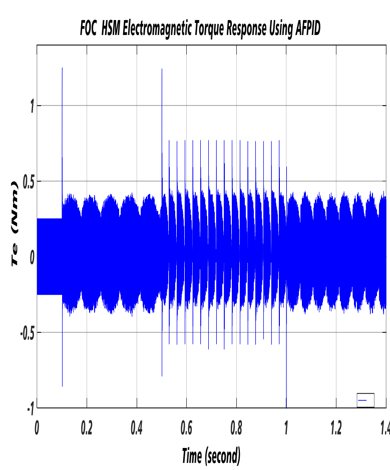

Figure 6: Torque response of variable speed HSM

Figure 6 depicts electromagnetic torque response of **the HSM** model, which reaches a steady-state value of about **0.4** Nm as the torque oscillates inside each step of rotor motion. The torque response shape is similar to the quadrature axis (Iq) current waveform in Figure 5 since Iq is directly proportional to the electromagnetic torque of HSM.

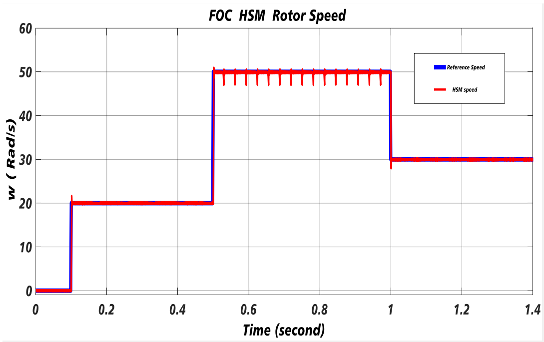

Figure 7: Rotor variable speed response of HSM

Figure 7 depicts the HSM rotor speed response to a variable step change in reference or command speed. During start-up at 0.1 sec, the motor speed rapidly reaches the reference speed value of 20 rad/s and tracks the reference speed until 0.5 second, when the reference speed changes to 50 rad/s, and also at 1.0 second, when the reference speed drops to 30 rad/s. Motor speed (red signal) tracks the reference (blue signal). The PID-Fuzzy controller exhibits good dynamic performance, with little overshoot and ripple occurring at higher speeds. This shows the effectiveness of the proposed closed-loop (FOC) control of the HSM drive system.

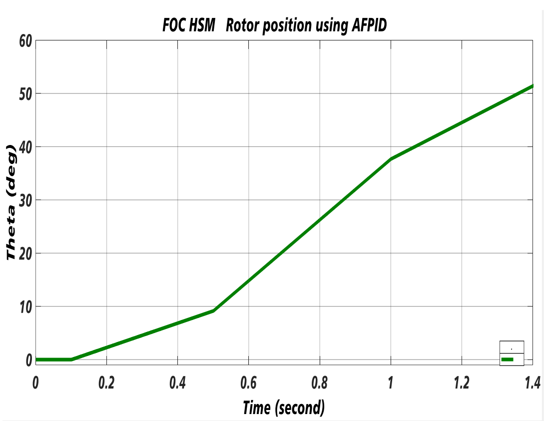

Figure 8: Rotor Position response to variable speed operation

Figure 8 demonstrates the HSM rotor position response in degrees to a variable step change in reference speed. (20 rad/s, 50 rad/s, and 30 rad/s) at 0.1 second, 0.5 second, and 1.0 second, respectively, where at these instances the corresponding step angles are 0-degree, 9.5 degree, and 38 degrees. And 51.5 degrees at 1.4 seconds.

4.2 Conventional PID-FOC Operation of Two-Phase Hybrid Stepper Motor

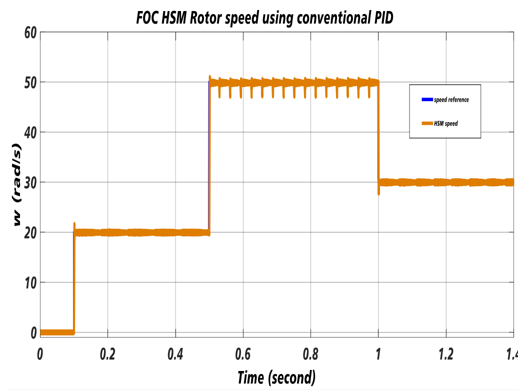

Figure 9 Rotor variable speed response of HSM using conventional PID

Figure 9 depicts the HSM rotor speed response to a variable step change in reference or command speed. During start-up at 0.1 sec, the motor speed rapidly reaches the reference speed value of 20 rad/s and tracks the reference speed until 0.5 seconds, when the reference speed changes to 50 rad/s, and also at 1.0 second, when the reference speed drops to 30 rad/s. Motor speed (red signal) tracks the reference (blue signal). Conventional PID controllers exhibit good dynamic performance, but there is more ripple during higher speed durations compared to Figure 7.

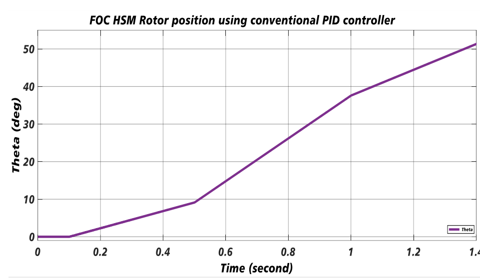

Figure 10: Rotor Position response to variable speed operation using conventional PID

Figure 10 demonstrates the HSM rotor position response in degrees to a variable step change in reference speed. (20 rad/s, 50 rad/s, and 30 rad/s) at 0.1 second, 0.5 second, and 1.0 second, respectively, is identical to Figure 8.

4. CONCLUSION

The hybrid stepper motor (HSM) was modelled and simulated in MATLAB/SIMULINK software to confirm the analysis in this work. The proposed closed-loop drive system was modelled based on field-oriented control (FOC) with an adaptive or Fuzzy-self-tuning PID controller. Reference speed was set at various values and simulated. From the simulation results verification. The proposed FOC drive model for HSM shows fast dynamic performance in both transient and steady-state operations as it takes little rise time, little overshoot, and zero steady-state error as the precision of position and speed level are high. However, at reference speeds higher than 90 rad/s (10 rad/s), they exhibit ripple and steady-state errors due to implementation errors and a lack of back-emf compensation. To overcome this limitation, motor parameters like winding inductance and resistance values must be adjusted. Also, PID controller gains should be tuned to achieve optimum speed response or precise position responses for higher-speed operation. The most suitable controller for stepper motor control depends on the availability of motor parameters

References

A. Okolo, C. C., Ekolo, K. U., Okwu, C. P., Suru, J. O. & Obinna, O. (2018) “Fuzzy logic controller Versus PID Controller (Dc Motor speed control)” International Journal for Research in Applied Science & Engineering Technology (IJRASET) Vol.6, Issue 4, pp 233-246.

B. Ong C. M. (1998) Dynamic simulation of Electric Machinery using Matlab/Simulink, Prentice Hall, Upper Saddle River.

C. Ormandzhiev, K. and Stanimir, Y. (2020). ‘’Design of Adaptive Fuzzy PID Controller for Electropneumatic Systems. E3S Web of Conference 207, 04002 (2020), pp1-8

D. Peng, Z., and Bi, C. (2019) Analysis of Drive Mode on Torque and Noise of Stepper Motor. Micromotors 2019, 52, 27–31.

E. Peng, Z.; Bi, C.; Yao, K.; Fang, L. (2021) Reducing acoustic noise of 3-phase hybrid stepper motor with drive mode. Electr. Eng. 2021, 103, 1–9. [CrossRef]

F. Abdelkarim, A. H. (2011). Control and Measuring Method for three phase Induction Motor with Improved Efficiency. Electronic and Information Technology, University of Darmstadt.

G. Acarnley, P. (2002). Stepping motors: A Guide Theory and Practice, 4th Edition. IEEE

H. Acarnley, P. "Stepping motors: a guide to modern theory and practice", Peter Peregrinus Ltd., I982.

I. Adepoju, G. A., Adeyemi, I. A., and Oni, O. (2014) Application of Fuzzy logic to the speed control of Dc Motor. International Journal of Engineering Trends and Technology (IJETT). 15(5), 215-218

J. Bendjedia, M., Ait-Amirat, Y., Walther, B., and Berthon, A. (2012). Position control of a sensorless stepper motor. IEEE Transactions on Power Electronics, 27(2), 578–587.

K. Bernardi, F., Carfagna, E., and Migliazza, G. (2022). Performance analysis of current control strategies for hybrid stepper motors. IEEE Open Journal of the Industrial Electronics Society, 3, 460-472.

L. Betin, F., Deloizy, M., and Goeldel, C. (1999). Closed loop control of steeping motor drive: comparison between PID control, Self-tuning regulation and fuzzy logic control. Journal of Eur. Power Electronic, 8(1-2), 33-39.

M. Betin, F., Pinchon, D., and Capolino, G. (2000). Fuzzy logic applied to speed control of a stepping motor drive. IEEE trans. Ind. Electron., 47(3), 610-622.

N. Chaber, P. M. (2019). Fast analytical model predictive controllers and their implementation for STM32 ARM microcontroller. IEEE Transactions on Industrial Informatics, 15(8), 4580-4590

O. Chunlei, W., and Dongxing, C. (2020). New Sensorless Speed Control of a Hybrid Stepper Motor Based on Fuzzy Sliding Mode Observer. Energies 2020, 13, 1-19.

P. Derammelaere, S, Debruyne, C., De Belie, F., Stockman, K., and Vandevelde, L. (2014). Load angle estimation for two-phase hybrid stepping motors. IET Electric Power Applications, 8(7), 257–266.

Q. Ehab, I., Mohamed, Z., and Mahmoud, K. (2011). DSP-Based Real-Time Control of a Two-Phase Hybrid Stepping Motor. International Electrical Engineering Journal (IEEJ) 1(1), 501-505

R. Fredriksen, T. (1968). Application of closed loop stepping motor, IEEE Trans. Automatic control, C-13, October, 464-474.

S. Hamid, N., Abdelrahim, A. and Ahmed, M. (2018). Developing the Hybrid Stepper Motor Model for Tracking Purpose Using New Methodology. In Proceedings of the International Workshop on Materials, Chemistry and Engineering (IWMCE 2018), pages 174-182 ISBN: 978-989-758-346-9.

T. Ikpe, A. E., Ikechukwu, O., and Paul, S. (2016). Comparative Analysis of a PID Controller using Ziegler –Nichols and Auto Tuning Method. International Academic Journal of Science and Engineering, 3(10), 1-16.

U. Kenjo, T. (2003). A stepping motors and microprocessor control, London, Oxford Clarendon press,

V. Kim, W., and Choo, C. (2011). Novel Position Detection Method for Permanent Magnet Stepper

Motors Using Only Current Feedback. IEEE Transactions on Magnetics, 47(10), 3590–3593.

W. Masi, A, Butcher, M. Martino, M. and Picatoste, R. (2012). An application of the extended Kalman filter for a sensorless stepper motor drive working with long cables," IEEE Transactions on Industrial Electronics. 59(11), 4217–4225.

X. Mohindru, P., Sharma, G., and Pooja, E. (2015). Simulation Performance of PID and Fuzzy logic controller for Higher order system. Communication on applied Electronics, 1(7), 31-35.

Y. Nilu, M., and Jebin, F. (2015). Simulation of Sensorless Position Control of a Stepper Motor with Field Oriented Control Using Extended Kalman Filter, International Journal of Innovative Research in Science, Engineering and Technology, 4(11), 10705-10710, 2015, DOI:10.15680/IJIRSET.2015.0410052.

Z. Peng Z and Chao Bi (2022) "A position senseless Closed-Loop Control Model of a Three-phase Hybrid Stepper Motor" Energies 2022, 15, 804 pp1-17

AA. Qais S. AL- Sabbagh and Ali Sabah Mahdi (2010) Pulse Width Modulation for High Performance Hybrid Stepper Motor 'Journal of Engineering Journal of Engineering, Number 4 Volume 16 December 2010, Pp 8206-8266

BB. Walz S, Lazar R, Buticchi G, et al. (2019)''Dahlin-based fast and robust current control of a PMSM in case of low carrier ratio. IEEE Access. 2019; 7:102199-102208.

CC. Yansuo, Z ,1,2 Leng Yonggang ,1 Lu Wenqi ,3 Li Yu,4 Li Qingmian,2 and Wu Di3 (2021) Research on a High-Speed and Heavy-Duty Closed-Loop Drive System of a Two-Phase Hybrid Stepping Motor Based on a Hybrid Controller, Hindawi Wireless Communications and Mobile Computing Volume 2021, Article ID 2515820, pp 1-13. https://doi.org/10.1155/2021/2515820

DD. Zaky. M.S, Ehap M. Ismaeil, Mahmoud M. Khater (2012) Gain Scheduling Adaptive Proportional-Integral Controller for a Field Oriented Control of Hybrid stepper Motor Drives. Electri Power Components and Systems. Taylor & Francis Group,LCC 40:777-791.

EE. Zhang X, Zhang L, Zhang Y. (2019) Model predictive current control for PMSM drives with parameter robustness improvement. IEEE Transactions on Power Electronics. 2019;34(2):1645-1657.

FF. Eke, A., Fischer, G., David, A., Ekpenyong, O., & EJ, A. The Effect of Rotor and Stator Slot Numbers on The Performance of Three-Phase Induction Motors Used for Transport Application.

GG. Sonolaa, M., Fischer, G., & Asuquo, E. Harmonic Analysis and Evaluation Of 52 Bus in Nigeria Transmission Network.